

Factors influencing the electrokinetic dispersion of PAH-degrading bacteria in a laboratory model aquifer

L. Shi · S. Müller · H. Harms · L. Y. Wick

Received: 31 January 2008 / Revised: 11 June 2008 / Accepted: 11 June 2008 / Published online: 8 July 2008
© Springer-Verlag 2008

Abstract Despite growing interest in the electro-bioremediation of contaminated soil it is still largely unknown to which degree weak electric fields influence the fate of contaminant-degrading microorganisms in the sub-surface. Here we evaluate the factors influencing the electrokinetic transport and deposition of fluorene-degrading *Sphingomonas* sp. LB126 in a laboratory model aquifer exposed to a direct current (DC) electric field (1 V cm^{-1}) typically used in electro-bioremediation measures. The influence of cell size, cell membrane integrity, cell chromosome contents (all assessed by flow cytometry), cell surface charge and cell hydrophobicity on the spatial distribution of the suspended and matrix-bound cells after 15 h of DC-treatment was evaluated. In presence of DC the cells were predominantly mobilised by electroosmosis to the cathode with an apparent velocity of 0.6 cm h^{-1} , whereas a minor fraction only of the cells augmented was mobilised to the anode by electrophoresis. Different electrokinetic behaviour of individual cells could be solely attributed to intra-population heterogeneity of the cell surface charge. In the absence of DC by contrast, a Gaussian-type distribution of bacteria around the point of injection was found. DC had no influence on the deposition efficiency, as the glass beads in presence and absence of an electric field retained quasi-equal fractions of the cells. Propidium iodide staining and flow cytometry analysis of the cells indicated the absence of negative influences of DC on the cell wall integrity of

electrokinetically mobilised cells and thus point at unchanged physiological fitness of electrokinetically mobilised bacteria.

Keywords Electro-bioremediation · Viability · PAH · *Sphingomonas* · Propidium iodide · Transport

Introduction

Engineered bioremediation of soil relies on the presence of contaminant-degrading bacteria and optimal physical and chemical conditions for their catabolic activity. In order to achieve substantial biodegradation, microorganisms must further come into contact with soil-bound contaminants, such as polycyclic aromatic hydrocarbons (PAHs). This may be a particular problem for bio-augmented organisms, which need to be transported to the zone of contamination (Thomas and Ward 1989). Numerous laboratory (Lahlou et al. 2000), field-scale (Dybas et al. 2002; Major et al. 2002) and modelling studies (Schafer et al. 1998; Shein et al. 2002; Kim 2006) have been performed to understand and predict microbial transport in porous media. The observed inefficiency of bacterial transport was attributed mainly to the extremely low hydraulic conductivity in soil micropores (Silliman et al. 2001) and bacterial attachment to the surfaces of soil particles (Baygents et al. 1998). Strategies such as the chemical modification of bacterial surfaces (Gross and Logan 1995) and treatment with surfactants (Jackson et al. 1994; Brown and Jaffe 2001) were proposed to enhance the efficiency of bacterial transport by decreasing bacterial attachment. However, at low hydraulic conductivity, bacterial transport will always be strongly limited (Li et al. 1996). In recent years, there has been increasing interest in electro-bioremediation, a hybrid

L. Shi · S. Müller · H. Harms · L. Y. Wick (✉)
Department of Environmental Microbiology,
UFZ Helmholtz Centre for Environmental Research,
Permoserstrasse 15,
04318 Leipzig, Germany
e-mail: lukas.wick@ufz.de

technology of bioremediation and electrokinetics, for the treatment of soil contaminated with hydrophobic organic compounds (HOC). Electrokinetics has the potential to enhance the contact probability of the bacteria and their HOC substrates by transporting bacteria to contaminant sources (Wick et al. 2007) or vice versa (Shi et al. 2008a).

Bacterial transport in porous media driven by electrokinetics has been reported. It is a result of either electrophoretic movement of negatively charged bacteria to the anode (DeFlaun and Condee 1997; Lee and Lee 2001) and/or bacterial migration with the electroosmotic water flow to the cathode (Sun and Romantschuk 2004; Wick et al. 2004). Besides this, differential electrophoresis in capillaries is an accepted method for the separation of bacteria in the laboratory (Rodriguez and Armstrong 2004). In comparison with hydraulic flow restricted by capillary effects, electrokinetics (i.e. electrophoresis and electroosmosis) are quite independent from pore size, and electroosmosis is especially efficient in fine-grained soils (with pores in the micrometer range or smaller) (Hlushkou et al. 2007). Here we present a study on the influence of an electric field typically used in electro-bioremediation (1 V cm^{-1}) on the transport and deposition of fluorene-degrading *Sphingomonas* sp. strain LB126 (van Herwijnen et al. 2003) in a model bench scale aquifer packed with glass beads. Total numbers of adhered and suspended cells were quantified at distinct distances from the injection point and analysed by flow cytometry for their cell size distribution, their membrane integrity (by propidium iodide (PI) uptake) and their chromosome contents indicating the cell cycle stage (by 4'-6-Diamidino-2-phenylindole (DAPI) staining). Static contact angle and dynamic light scattering experiments were performed to assess the influence of electric field on the physico-chemical cell surface characteristics (cell surface hydrophobicity and cell surface charge) for the transport behaviour of the bacteria (Redman et al. 2004).

Materials and methods

Organisms and culture conditions *Sphingomonas* sp. LB126 was cultivated in minimal medium (Harms and Zehnder 1994) with 1.0 g L^{-1} glucose as sole carbon and energy source. A previous study (van Herwijnen et al. 2003) has shown that strain LB126 is also able to grow on fluorene. Cultures were grown at room temperature ($20 \text{ }^\circ\text{C}$) on a gyratory shaker at 150 rpm in 500 mL Erlenmeyer flasks containing 300 mL of medium. Growth together with stages in the cell cycle (via DNA contents as a measure of chromosome numbers) and membrane integrity (via uptake of propidium iodide, PI) were assessed by flow cytometry as described earlier (Shi et al. 2007). Cultures were harvested in the early stationary phase after 24 h of growth,

washed three times in 50 mM Tris acetate buffer (TA) at $\text{pH}=7.0$, and re-suspended and concentrated in TA to obtain highly concentrated bacterial inocula (optical density $\text{OD}_{578 \text{ nm}} \approx 0.30$) for use in electrokinetic experiments. No growth of strain LB126 on TA buffer was detected in independently performed batch cultures (initial OD of ca. 0.1) run for 24 h.

Electrokinetic experiments The apparatus used in electrokinetic experiments has been described in detail earlier (Wick et al. 2004). Shortly, it consists of two electrode chambers ($2 \times 7 \times 3.5 \text{ cm}$) at the ends, a lid-covered model aquifer chamber ($35.5 \times 4 \times 3.5 \text{ cm}$) in between and a bypass channel below the aquifer chamber having hydraulic contact with both electrode chambers to exclude advective hydraulic water flow through the aquifer chamber. The whole chamber was filled with 0.05 M Tris-acetate-buffer of $\text{pH} 7$ and the electrolyte in both electrode chambers was recirculated to a common 1-L reservoir of TA buffer at a flow rate of 120 mL h^{-1} with a peristaltic pump to avoid any pH changes in the electrode chambers and the electrokinetic chamber during the experiments (Wick et al. 2004). Glass beads of 1 mm in diameter (Roth AG, Reinach, Switzerland) were sterilised, carefully packed into the aquifer chamber and then saturated by TA buffer (porosity, 0.39). In presence of an electric DC-field, the glass beads allowed for an electroosmotic permeability coefficient of $2.1 \times 10^{-8} \text{ m}^2 \text{ V}^{-1} \text{ s}^{-1}$ (Wick et al. 2004). The use of a model aquifer with well-defined properties (surface charge and ionic strength) is very crucial for the fundamental discussions in this study. One milliliter of bacterial inoculum was slowly injected during 1 min at half of the bed depth at equal distance from the two electrodes in the centre of the aquifer chamber. A constant electric field strength of 1 V cm^{-1} was applied for 15 h with an initial current density (J) between the electrodes of $J=1.8 \text{ mA cm}^{-2}$. At the end of each experiment pore water samples were taken simultaneously from the aquifer chamber at the point of injection (0 cm), and at 4.5, 9, and 15 cm towards both electrodes. At each sampling point, 10 mL of pore water and a sample of about 12 mL glass beads were harvested as described earlier (Wick et al. 2004). Harvested glass beads were re-suspended in 20 mL 50 mM TA in a sterilised test tube and sonicated two times for 30 s with a break in between to detach adhered bacteria. After the detachment of bacteria the beads were dried and weighed to calculate exact bead surface areas of the samples. All bacterial suspensions were further analysed as described below.

The efficiency of detachment was tested in a separate column system. LB126 cells were first pumped through a column packed with the same type of glass beads and the percentage of adhered cells was calculated from the

breakthrough curve. Afterwards the glass beads were harvested and cells were detached following the same method as in the electrokinetic experiments. About $24 \pm 8\%$ of cells adhered to glass beads could be detached with the above-mentioned method. This detachment efficiency was used to estimate the total amount of cells adhered on glass beads during electrokinetic and control treatments.

Multiparametric flow cytometry analyses Flow cytometry measurements were carried out using a MoFlo (Dako, Fort Collins, CO, USA) equipped with two water-cooled argon-ion lasers (Innova 90C and Innova 70C from Coherent, Santa Clara, CA, USA). Excitation of 580 mW at 488 nm was used to analyse the forward scatter and side scatter as trigger signals at the first observation point. The orthogonal signal was first reflected by a beam-splitter and then recorded after reflection by a 555 nm long-pass dichroic mirror, passage by a 505 nm short-pass dichroic mirror and a BP 488/10. DAPI fluorescence was passed through a 450/65 band pass filter, green fluorescence through BP 520/15 and red fluorescence through BP620/45. Photomultiplier tubes were obtained from Hamamatsu Photonics (models R 928 and R 3896; Hamamatsu City). Fluorescent beads (yellow-green fluorescent beads: 2 μm , FluoSpheres 505/515, F-8827; blue fluorescent beads: 1 μm , FluoSpheres 350/440, F-8815; crimson fluorescent beads: 1 μm , FluoSpheres 625/645, F-8816; Invitrogen, USA) were used to align the MoFlo. Also, an internal DAPI-stained bacterial cell standard was used to achieve distributions with a coefficient of variation less than 6%. Amplification was carried out at logarithmic scales. Data were acquired and analysed using the Summit software (Dako, Fort Collins, CO, USA).

- **Cell Counting.** The numbers of cells were counted accurately (as seen from negligible deviation) using flow cytometry. Fluorescent beads (FluoSpheres[®] polystyrene microspheres 1.0 μm in diameter, yellow-green fluorescent (505/515), Invitrogen) were mixed with 1 mL of samples taken from electrokinetic experiments. Dot plots were gated with regard to cell populations and beads, and then the numbers of cells were calculated (Vogt et al. 2005). Cell aggregation was observed neither by microscopy nor by flow cytometry, so clearly separated sub-populations were analysed.
- **Membrane integrity.** Cells with compromised membranes were quantified by flow cytometry using the nucleic acid specific fluorochrome propidium iodide. Details of the staining procedure have been presented elsewhere (Shi et al. 2007). Ten microLiters PI (SIGMA-ALDRICH, Steinheim, Germany; final concentration 1.05 μM , stock solution 0.07 mg mL^{-1} PBS, pH 7.2) were mixed immediately with 1 mL of samples

taken from electrokinetic experiments (directly out of the chamber). After 10 min of staining, samples were measured by flow cytometry. The fractions (%) of red PI-stained cells were determined.

- **DNA-patterns.** The harvested cells were centrifuged at $3,200 \times g$ for 5 min, inactivated with 10% NaN_3 and stored at 4 °C for at least 2 h. DNA patterns of preserved cells were then obtained in the following way: 2 mL of diluted cell suspension were treated with 1 mL solution A (2.1 g citric acid/0.5 g Tween 20 in 100 mL bidistilled water) for 10 min, washed and re-suspended in 2 mL solution B (0.24 μM 4',6-diamidino-2'-phenylindole [DAPI, Sigma], 400 mM Na_2HPO_4 , pH 7.0) for at least 20 min in the dark at room temperature using a modification of a standard procedure (Meistrich et al. 1978).

Determination of physico-chemical surface properties of bacterial cells and glass beads Cell surface hydrophobicity of bacteria taken from electrokinetic experiments were derived from the static contact angles (θ_w) of small water droplets placed on filters covered with layers of bacteria. Measurements were performed with a goniometer microscope (Krüss GmbH, Hamburg, Germany) as described before (Wick et al. 2002). Contact angles of at least 10 droplets of 1 μL each were measured. The zeta potential (ζ) was approximated from the electrophoretic mobility of the bacteria in 50 mM TA measured by a Doppler electrophoretic light scattering analyzer (Zetamaster, Malvern Instruments, Malvern, UK) according to the method of Helmholtz–Smoluchowski (Hiementz 1986). The zeta-potential of glass beads was approximated by the same method. Prior to the measurements, the glass beads were levitated to form a colloidal suspension (Qiu and Ling 2006) in 50 mM Tris acetate buffer (TA) at pH=7.0.

Bacterial diffusion: The Einstein–Smoluchowski law (Eq. 1) relates the mean-squared displacement $\langle x^2 \rangle$ (cm^2) over a time interval t (h) to the effective diffusion coefficient D_{eff} ($\text{cm}^2 \text{h}^{-1}$).

$$\langle x^2 \rangle = 2 \times D_{\text{eff}} \times t \quad (1)$$

The mean transport velocity u_{dif} (cm h^{-1}) can be estimated by Eq. 2:

$$u_{\text{dif}} = \frac{\langle x \rangle}{t} \quad (2)$$

Electrokinetic-transport: The overall electrokinetic mobility μ_{EK} ($\text{cm}^2 \text{V}^{-1} \text{h}^{-1}$) of bacteria (Eq. 3) is the resultant of

their electrophoretic (μ_{EP}) (Eq. 4) and electroosmotic (μ_{EO}) (Eq. 5) mobilities according to

$$\mu_{EK} = \mu_{EO} + \mu_{EP} \quad (3)$$

$$\mu_{EP} = \frac{\varepsilon_r \varepsilon_0 \zeta_{bac}}{\eta} \quad (4)$$

$$\mu_{EO} = \frac{\varepsilon_r \varepsilon_0 \zeta_{soil}}{\eta} n \tau \quad (5)$$

where ε_r is the dielectric constant of water ($\varepsilon_r=78.5$), ε_0 ($1.15 \times 10^{-2} \text{ kg cm h}^{-2} \text{ V}^{-2}$) is the vacuum permittivity, η ($3.19 \times 10^{-2} \text{ kg cm}^{-1} \text{ h}^{-1}$) is the viscosity of water, ζ_{soil} (V) is the mean zeta potential of the model soil matrix (in our case glass beads) and ζ_{bac} (V) is the mean zeta potential of LB126 cells in 50 mM TA buffer; n (0.39) and τ (1.8) are the porosity and tortuosity (Kohlmeier et al. 2005) of the glass bead, respectively. Using these calculated values of μ_{EP} and μ_{EO} , the theoretical electrokinetic velocity u_{EK} (cm h^{-1}) can be estimated from

$$u_{EK} = \mu_{EK} \times E \quad (6)$$

where E (V cm^{-1}) is the electric field strength applied.

Bacterial deposition: The apparent bacterial partition ratio R_d (Eq. 7) relates the number of freely suspended cells (C_{pw}) at given distances (d) from the point of injection to the number of deposited cells (C_{gb}) in the corresponding volume of total porous medium.

$$R_d = \frac{C_{pw}(d)}{C_{gb}(d)} \quad (7)$$

Bacterial deposition efficiency (D_d) (Eq. 8) is the concentration of deposited bacteria at distance (d) relative to the number of cells having passed this location during the elapsed time (15 h) of the experiment.

$$D_d = \frac{C_{gb}(d)}{\int_d^{15} (C_{pw}(d) + C_{gb}(d)) dd} \quad (8)$$

Results

Influence of weak DC-electric fields on bacterial transport No directed movement of the bacteria occurred in the absence of DC. The distribution of the cell abundance at the point of injection after 15 h (Fig. 1a, open circles) was fitted best by a diffusion-driven Gaussian distribution ($R^2=0.9832$) (Fig. 1a, solid line). Assuming Gaussian distribution an effective diffusion coefficient (D_{eff}) of $0.15 \text{ cm}^2 \text{ h}^{-1}$ and a mean transport velocity u_{diff} of 0.13 cm h^{-1} can be calculated (Eqs. 1 and 2). However, when *Sphingomonas* sp LB126 cells were exposed to an electric field of 1 V cm^{-1} directed displacement of the bacteria towards the cathode (Fig. 1b) was observed. Estimates based on the peak displacement (9 cm) after 15 h of DC-application revealed an approximate mean electrokinetic transport velocity of -0.6 cm h^{-1} . Figure 1b clarifies the electrokinetic influence on bacterial dispersion by depicting the ratios of electrokinetically- and diffusion-driven cells: Electroosmosis led to an up 24-fold and a twofold increase of suspended and surface-bound cells relative to the control at the expense of a significant (fivefold of suspended cells) reduction of cells at the injection point. Despite of the electroosmotic

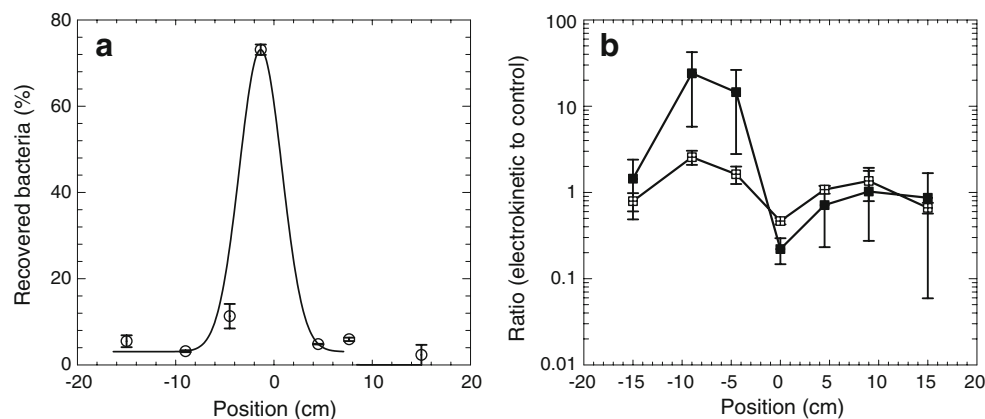


Fig. 1 **a** Gaussian-fit (solid line) of the relative distribution of *Sphingomonas* sp. LB126 recovered from the model aquifer after the injection of about 3×10^{10} cells mL^{-1} in the absence of DC (open circles). **b** Numbers of free (filled squares) and surface-bound cells (open squares) of strain LB126 cells after exposure to 1 V cm^{-1} for

15 h relative to free and surface-bound cells recovered in the control experiment. Negative distances direct towards the cathode while positive to anode. Figure 1 represents averages and standard deviations of ≥ 3 independent experiments

predominance, a minor yet statistically significant fraction of the LB126 cells was mobilised by electrophoresis to the anode as seen by ratios above unity of adhered cells in the anode compartment.

Influence of weak DC-electric fields on bacterial deposition Significant differences of apparent bacterial partition ratios R_d (Eq. 7) of DC-exposed and control cells were observed (Fig. 2a). At the point of injection ($d=0$), R_d of cells in the control was threefold higher than R_d of DC-exposed cells (Fig. 2a). In contrast, at the cathode side an up to fourfold-enhanced R_d ($d=-9$ cm) in presence of DC was observed, whereas no differences of R_d of cells at the anode side was observed. In order to account for the fact that R_d is influenced by the deposition history, i.e. that C_{gb} is the reflection of both the deposition efficiency and the elapsed time available for deposition; we further calculated the deposition efficiency (D_d) as explained in Eq. 8. Results in Fig. 2b show that the elevated R_d of cells transported by electroosmosis (Fig. 2a) was not reflected by D_d . The calculated variations of D_d of ranging from 0.11–0.21 (Fig. 2b) were statistically (student *t*-test) not significant and thus point at the absence of an effect of electrokinetic mobilisation on bacterial deposition.

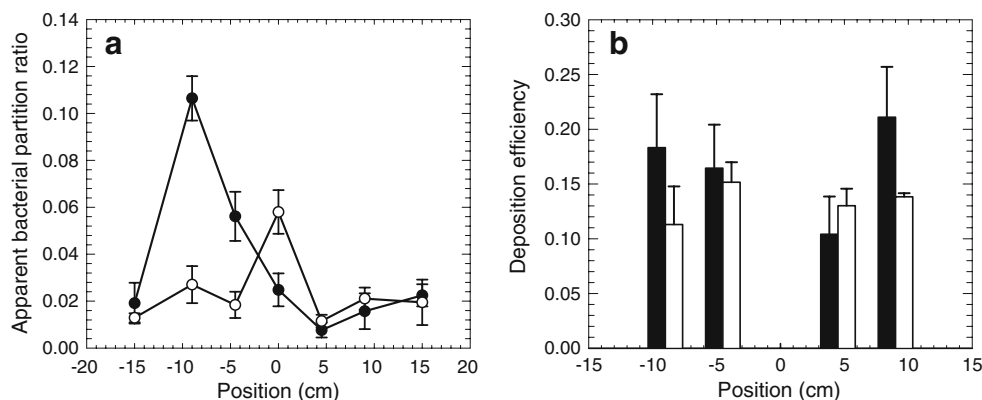
Influence of intra-population heterogeneity on electrokinetic dispersion In order to explain the observation that a fraction of the population of strain LB126 was transported to the anode (visible as a hump-shaped peak in the anode half of Fig. 1b), the potential role of intra-population cell heterogeneities on electrokinetic mobilisation was tested. Bacteria were sampled at distinct locations in the model aquifer after electrokinetic treatment and subsequently analysed for their cell sizes, membrane integrity, chromosome contents, and the charge and hydrophobicity of their cell surfaces. We observed uniform cell surface hydrophobicity ($\Theta_w = 40.6 \pm 4.1^\circ$) and cells size (length=1.2 μm , width=1 μm) regardless of the treatment and the location sampled. Likewise, cells from DC and control treatments

retrieved from all locations exhibited DNA patterns identical to the inoculum (data not shown). On average 83% and 17% of the cells possessed one chromosome and two chromosome contents, respectively. The mean zeta potential ($\zeta = -2.9 \pm 6.9$ mV) of the LB126 inoculum was derived from electrophoretic mobility measurements by dynamic light scattering (DLS) (Fig. 3a). Interestingly, significant differences in the zeta potentials of cells along the aquifer were also found after DC treatment (Fig. 3b). Cells transported toward the anode were more negatively charged than cells transported toward the cathode (Fig. 3b). In contrast, cells transported purely by diffusion and random movement in control experiment had more or less the same zeta potential and only cells remaining at the injection point presented a significantly higher zeta potential (Fig. 3b). No correlation was observed between the cell surface charge and the integrity of the bacteria (inferred from intact membranes resisting against PI uptake (Shi et al. 2008b) after 15 h of electrokinetic treatment (Table 1). The average PI-stained fraction (PI-%) of mobilised bacteria was 1.3% irrespective of DC application, which is slightly below the PI-% of the inoculum (2.3%). By contrast, increased PI-% of 15 and 7% (Table 1) were found at the injection points after DC-treatment and control experiments, respectively.

Discussion

Effect of the weak DC-electric fields on the dispersion and deposition of *Sphingomonas sp.* LB126 Dispersion of a non-growing population of bacteria in a porous medium around the point of injection is the result of bacterial transport that is counteracted by deposition processes. Transport mechanisms may include bacterial movement, diffusion, and hydraulic advection. In this study, we purportedly excluded hydraulic flow in order to simplify the study of physical factors influencing the electrokinetic

Fig. 2 Apparent bacterial partition ratios (R_d , **a**) and deposition efficiencies (D_d , **b**) of electrokinetically mobilised (filled symbols and columns) and control cells (open symbols and columns). Negative distances direct towards the cathode while positive to anode. Figure 2 represents average and standard deviations of ≥ 3 independent experiments



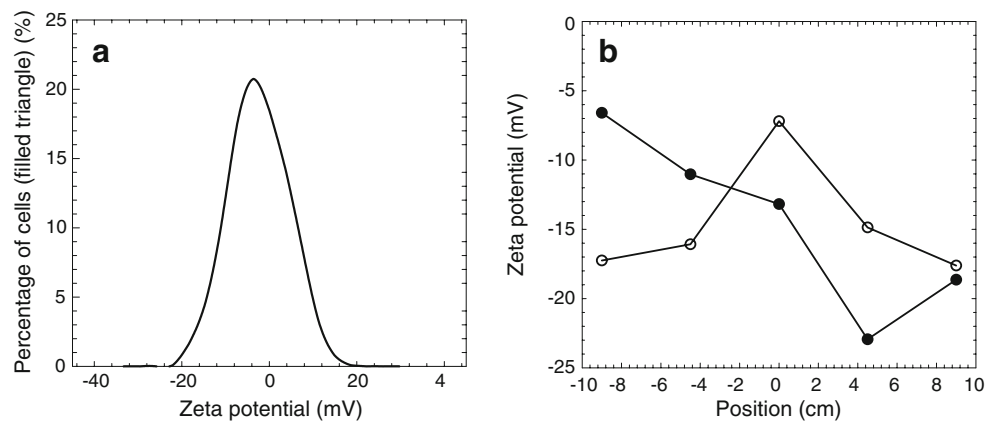


Fig. 3 **a** Representative distribution of the zeta potential (ζ) of an axenic culture of *Sphingomonas* sp. LB126 as calculated from dynamic light scattering (DLS) experiments. The distribution is a result of the Brownian motion, heterogeneity of surface structure and

surface charge of the bacteria. **b** Representative distribution of the ζ of cells harvested along the aquifer in presence (filled circles) or absence (open circles) of an electric field strength of ($E=1 \text{ V cm}^{-1}$) for 15 h. Negative distances direct towards the cathode while positive to anode

transport of *Sphingomonas* sp. LB126. The Gaussian distribution of strain LB126 abundance around the injection point (Fig. 1a, solid line) in the absence of a DC-electrical field indicates that diffusive random movement of bacteria were the only translocation mechanisms. At a circum-neutral pH, bacteria (Wilson et al. 2001) and mineral particles (Saichek and Reddy 2005) are typically negatively charged. In an electric field applied to porous media the random movement and diffusion of negatively charged bacteria will thus be superimposed by electrophoresis and electroosmosis acting in opposite directions. The observed mean transport velocity ($u_{EK}=-0.6 \text{ cm h}^{-1}$) of LB126 cells in our model soil matrix was clearly dominated by electroosmosis and as a such about fivefold increased relative to diffusion-driven dispersion ($u_{dif}=0.13 \text{ cm h}^{-1}$) yet similar to the electroosmotic movement of uncharged molecular markers (Wick et al. 2004) and the theoretically

predicted value (u_{EK}) of -0.82 cm h^{-1} , which was calculated based on the mean zeta potential (ζ_{soil}) of the glass bead surface ($\zeta_{soil}=-45.7 \text{ mV}$), the ζ_{bac} of LB126 cells (-2.94 mV) (Eq. 6), the observed electrophoretic ($\mu_{EP}=0.08 \text{ cm}^2 \text{ V}^{-1} \text{ h}^{-1}$), and the electroosmotic mobility ($\mu_{EO}=-0.90 \text{ cm}^2 \text{ V}^{-1} \text{ h}^{-1}$) of LB126 cells (Eqs. 4 and 5) at the experimental conditions used, respectively. The bacterial deposition efficiency (D_d) and the apparent bacterial partition ratio (R_d) were further calculated to assess the influences of electroosmotic, electrophoretic and diffusive transport mechanisms on the deposition of mobilised cells. Similar values of D_d of both control and electrokinetically treated LB126 cells (Fig. 2b) however, indicated no apparent influence of electrokinetic transport on deposition of strain LB126 relative to purely diffusion-driven transport (D_{eff} of $0.15 \text{ cm}^2 \text{ h}^{-1}$). D_{eff} is in the range of typical bulk random motility diffusion coefficients derived from capillary experiments ($0.005-0.248 \text{ cm}^2 \text{ h}^{-1}$) (Lewus and Ford 2001).

Table 1 Influence of electrokinetic mobilisation on the permeability of *Sphingomonas* sp. LB126 cell membranes for propidium iodide (PI) as a potential indicator of the impact of weak electric fields on cell fitness

Electric field strength (V cm^{-1})	Position (cm)	Cells stained by PI (%)	
		PW	GB
control (0)	-4.5 to -15 cm	1.8 ± 2.0	0.9 ± 0.2
	Point of injection (0 cm)	0.9 ± 0.7	7.1 ± 2.0
	4.5 to 15 cm	1.1 ± 1.3	1.2 ± 0.3
1	Cathode half (-4.5 to -15 cm)	1.1 ± 0.6	1.4 ± 0.6
	Point of injection (0 cm)	15.5 ± 2.6	10.8 ± 2.8
	Anode half (4.5 to 15 cm)	1.6 ± 1.6	1.1 ± 0.3

PI-uptake was assessed for cells retrieved from pore water (PW) and cells detached from glass beads (GB). The PI-% (percentage of PI stained cells) of the injected cells was $2.3 \pm 0.4\%$

The difference between D_d and R_d can be explained by the fact that R_d is influenced by the deposition history, i.e. that C_{gb} is the reflection of both the deposition efficiency and the elapsed time available for deposition. The high R_d at cathode side in presence of DC represents a snapshot of the efficient electroosmotic displacement of the not-yet-deposited fraction of the injected population as reflected clearly in Fig. 1b. Surprising in Fig. 1b however is, that free and surface-bound cells in the anode half were nearly as abundant as in the control experiment. Seen the strong overall displacement of the population toward the cathode, this is astonishing and indicates that part of the population may have undergone higher electrophoretic attraction to the anode than the mean population. This observation motivated us to analyse the influence of population heterogeneity on the electrokinetic dispersion of bacteria in soil matrix.

Influence of population heterogeneity on electrokinetic transport Heterogeneity in pure bacterial population and its significance for bacterial transport and attachment in porous media have been recognised and discussed before (Simoni et al. 1998; Bolster et al. 2000; van der Mei and Busscher 2001; Mailloux et al. 2003). For strain LB126 we observed uniform cell surface hydrophobicity, cell size, and chromosome content regardless of the treatment and the location sampled. By contrast, significant differences in the zeta potentials of electrokinetically-mobilised cells along the aquifer were detected. Cells transported by electrophoresis toward the anode were more negatively charged than cells translocated by electroosmosis toward the cathode (Fig. 3b). No differences in the zeta potential of diffusively transported cells however were observed in the control. The zeta potential of the cells was derived from electrophoretic mobility measurements by dynamic light scattering (DLS). Experimental values were subsequently used in Eq. 4 for the calculation of the electrophoretic component of the bacterial transport. Closer inspection of the DLS results of the inoculum (Fig. 3a) revealed a Gaussian-type distribution of individual zeta potential signals ranging from $\zeta_{bac} = -22.1$ mV to $\zeta_{bac} = 18.6$ mV and thus points at an intra-population heterogeneity of the cell surface charge of the inoculum. In order to avoid over-interpretation of this finding however, it should be noted that the DLS signal width can also be partially caused by the limitations in the precision of the determination (e.g. the Brownian motion of the cells and their variations in size or cell surface structure) (Xu 1993; van der Mei and Busscher 2001; Dong 2002). Given the intra-population heterogeneity in the zeta potential and the continuously increasing cell surface charges towards the anode (Fig. 3b, filled circles), one may derive that the model aquifer, similar to capillary electrophoresis, separated individual bacteria according to their surface charge during electrokinetic treatment. It thus appears that electrophoresis compensated electroosmosis as mobilising force and consequently resulted in an apparent translocation of more negatively charged bacteria to the anode. In order to theoretically over-compensate electroosmotic forces (Eq. 5) by electrophoresis (Eq. 4), a zeta potential of -30 mV of the cells would have been required rather than the observed maximum of -22.1 mV. Nevertheless similar fractions of the total population were transported towards the anode in presence or absence of an applied electric field. This indicates that for part of the sub-population electroosmosis was just compensated by electrophoresis and that diffusion may account for the translocation in our system. It also may be that heterogeneities of the electroosmotic flow in the glass bead allowed electrophoresis to compensate the electroosmotic translocation of part of the more negatively charged sub-population. It was also interesting to see, that in control

experiments allowing for diffusion of the cells only, bacteria with higher negative zeta potentials tended to move further, leaving a sub-population of less negative zeta potentials at the injection point behind (Fig. 3b, open circles). This can be explained by favoured deposition (i.e. more retardation) of less negatively (less electrostatic repulsion) bacteria (Poortinga et al. 2002). Similar to the zeta potential, a clearly enhanced PI-% of LB126 cells at the point of injection was observed (Table 1). Increases were up to three- and sevenfold in the control and DC-treated experiment, respectively. High PI-% however was observed for cells remaining at the point of injection only. The PI-% of all mobilised (either by diffusion or electrokinetic processes) was consistently smaller than the value of the inoculum (Table 1). This surprising observation can be convincingly explained by a rough mass-balance calculation assuming that: (1) the total number of PI-stainable cells added by the inoculum (2–3%) kept unchanged after 15 h of electrokinetic experiments; (2) only PI-unstainable cells were transported away from the injection point (for unknown reasons); and (3) thereby simply PI-stainable cells were concentrated at the injection point (Shi et al. 2008b). Interestingly in the control experiment, only attached bacteria exhibited significantly enhanced PI-% (Table 1), which suggests better PI-staining of adhered cells. It should be noted that PI-incorporation into environmental bacteria does not necessarily reflect reduced viability (Shi et al. 2007). We recently observed that even actively growing *Sphingomonas* sp. LB126 bacteria were stained by PI and remained culturable on LB-agar plates (Shi et al. 2007). However, no growth was supposed to be possible during 15 h of experiments in TA buffer and no difference of DNA pattern was observed between the cells harvested at injection point and mobilised cells, and hence the active growth of LB126 cells only at injection point seems less possible. As the overall PI-% of electrokinetically mobilised bacteria was below 2% in this study, it appears that a weak DC electric field does not affect the integrity of electrokinetically transported bacteria.

Relevance for electro-bioremediation This work demonstrates that electrokinetics in presence of 1 V cm^{-1} of electric field can transport bacteria at velocities up to $0.4\text{--}0.8 \text{ cm h}^{-1}$ in coarse porous media with transport heavily depending on the physico-chemical properties of both the porous media and the surface properties of individual bacteria and confirms earlier data as has been summarised recently (Wick et al. 2007). The results also demonstrate that minor heterogeneities of bacterial populations may have an important effect on the distribution of microorganisms. Although a pure culture was used in this study, it mimics the electrokinetic transport behaviour of differently charged sub-surface bacteria. Given the right con-

ditions and organisms, electrokinetic dispersion could thus be used to distribute specialised bacteria in hotspots of contamination, e.g. in aquifer sediments. To our knowledge, this is the first study that indicates the absence of electrokinetic effects on the deposition efficiency of bacteria in (model) soil matrices. The observation that electrokinetically transported bacteria of strain LB126 exhibited very low permeability for propidium iodide (as a cell integrity indicator) is promising in the perspective of utilizing catabolically active bacteria under mild electrokinetic conditions.

Acknowledgements The authors wish to thank H. Engewald, T. Hübschmann, J. Reichenbach, R. Remer, C. Süring and B. Würz for skilled technical assistance.

References

- Baygents JC, Glynn JR, Albinger O, Biesemeyer BK, Ogden KL, Arnold RG (1998) Variation of surface charge density in monoclonal bacterial populations: implications for transport through porous media. *Environ Sci Technol* 32:1596–1603
- Bolster CH, Mills AL, Hornberger G, Herman J (2000) Effect of intra-population variability on the long-distance transport of bacteria. *Ground Water* 38:370–375
- Brown DG, Jaffe PR (2001) Effects of nonionic surfactants on bacterial transport through porous media. *Environ Sci Technol* 35:3877–3883
- DeFlaun MF, Condee CW (1997) Electrokinetic transport of bacteria. *J Hazard Mater* 55:263–277
- Dong HL (2002) Significance of electrophoretic mobility distribution to bacterial transport in granular porous media. *J Microbiol Methods* 51:83–93
- Dybas MJ, Hyndman DW, Heine R, Tiedje J, Linning K, Wiggert D, Voice T, Zhao X, Dybas L, Criddle CS (2002) Development, operation, and long-term performance of a full-scale biocurtain utilizing bioaugmentation. *Environ Sci Technol* 36:3635–3644
- Gross MJ, Logan BE (1995) Influence of different chemical treatments on transport of *alcaligenes paradoxus* in porous-media. *Appl Environ Microbiol* 61:1750–1756
- Harms H, Zehnder AJB (1994) Influence of substrate diffusion on degradation of dibenzofuran and 3-chlorodibenzofuran by attached and suspended bacteria. *Appl Environ Microbiol* 60:2736–2745
- Hiementz PC (1986) Principles of colloid and surface chemistry. Dekker, New York
- Hlushkou D, Khirevich S, Apanasovich V, Seidel-Morgenstern A, Tallarek U (2007) Pore-scale dispersion in electrokinetic flow through a random sphere packing. *Anal Chem* 79:113–121
- Jackson A, Roy D, Breitenbeck G (1994) Transport of a bacterial suspension through a soil matrix using water and an anionic surfactant. *Water Res* 28:943–949
- Kim SB (2006) Numerical analysis of bacterial transport in saturated porous media. *Hydrol Processes* 20:1177–1186
- Kohlmeier S, Smits THM, Ford RM, Keel C, Harms H, Wick LY (2005) Taking the fungal highway: mobilization of pollutant-degrading bacteria by fungi. *Environ Sci Technol* 39:4640–4646
- Lahlou M, Harms H, Springael D, Ortega-Calvo JJ (2000) Influence of soil components on the transport of polycyclic aromatic hydrocarbon degrading bacteria through saturated porous media. *Environ Sci Technol* 34:3649–3656
- Lee HS, Lee K (2001) Bioremediation of diesel-contaminated soil by bacterial cells transported by electrokinetics. *J Microbiol Biotechnol* 11:1038–1045
- Lewus P, Ford RM (2001) Quantification of random motility and chemotaxis bacterial transport coefficients using individual-cell and population-scale assays. *Biotechnol Bioeng* 75:292–304
- Li BL, Loehle C, Malon D (1996) Microbial transport through heterogeneous porous media: random walk, fractal, and percolation approaches. *Ecol Model* 85:285–302
- Mailloux BJ, Fuller ME, Onstott TC, Hall J, Dong HL, DeFlaun MF, Stregler SH, Rothmel RK, Green M, Swift DJP, Radke J (2003) The role of physical, chemical, and microbial heterogeneity on the field-scale transport and attachment of bacteria. *Water Resour Res* 39:1142
- Major DW, McMaster ML, Cox EE, Edwards EA, Dworzatzek SM, Hendrickson ER, Starr MG, Payne JA, Buonamici LW (2002) Field demonstration of successful bioaugmentation to achieve dechlorination of tetrachloroethene to ethene. *Environ Sci Technol* 36:5106–5116
- Meistrich ML, Gohde W, White RA, Schumann J (1978) Resolution of x-spermatids and y-spermatids by pulse cytophotometry. *Nature* 274:821–823
- Poortinga AT, Bos R, Norde W, Busscher HJ (2002) Electric double layer interactions in bacterial adhesion to surfaces. *Surf Sci Rep* 47:3–32
- Qiu YP, Ling F (2006) Role of surface functionality in the adsorption of anionic dyes on modified polymeric sorbents. *Chemosphere* 64:963–971
- Redman JA, Walker SL, Elimelech M (2004) Bacterial adhesion and transport in porous media: Role of the secondary energy minimum. *Environ Sci Technol* 38:1777–1785
- Rodriguez MA, Armstrong DW (2004) Separation and analysis of colloidal/nano-particles including microorganisms by capillary electrophoresis: a fundamental review. *J Chromatogr B-Anal Technol Biomed Life Sci* 800:7–25
- Saichek RE, Reddy KR (2005) Electrokinetically enhanced remediation of hydrophobic organic compounds in soils: a review. *Crit Rev Environ Sci Technol* 35:115–192
- Schafer A, Ustohal P, Harms H, Stauffer F, Dracos T, Zehnder AJB (1998) Transport of bacteria in unsaturated porous media. *J Contam Hydrol* 33:149–169
- Shein EV, Polyanskaya LM, Devin BA (2002) Transport of microorganisms in soils: physicochemical approach and mathematical modelling. *Eurasian Soil Sci* 35:500–508
- Shi L, Günther S, Hübschmann T, Wick LY, Harms H, Müller S (2007) Limits of propidium iodide (PI) as a cell viability indicator for environmental bacteria. *Cytometry Part A* 71:592–598
- Shi L, Harms H, Wick LY (2008a) Electroosmotic flow stimulates the release of alginate-bound phenanthrene. *Environ Sci Technol* 42:2105–2110
- Shi L, Muller S, Harms H, Wick LY (2008b) Vulnerability of electrokinetically dispersed PAH-degrading bacteria in a model aquifer. *Environ Geochem Health* 30:177–182
- Silliman SE, Dunlap R, Fletcher M, Schneegurt MA (2001) Bacterial transport in heterogeneous porous media: observations from laboratory experiments. *Water Resour Res* 37:2699–2707
- Simoni SF, Harms H, Bosma TNP, Zehnder AJB (1998) Population heterogeneity affects transport of bacteria through sand columns at low flow rates. *Environ Sci Technol* 32:2100–2105
- Suni S, Romantschuk M (2004) Mobilisation of bacteria in soils by electro-osmosis. *FEMS Microbiol Ecol* 49:51–57
- Thomas JM, Ward CH (1989) In situ bioremediation of organic contaminants in the subsurface. *Environ Sci Technol* 23:760–766
- van der Mei HC, Busscher HJ (2001) Electrophoretic mobility distributions of single-strain microbial populations. *Appl Environ Microb* 67:491–494

- van Herwijnen R, Wattiau P, Bastiaens L, Daal L, Jonker L, Springael D, Govers HAJ, Parsons JR (2003) Elucidation of the metabolic pathway of fluorene and cometabolic pathways of phenanthrene, fluoranthene, anthracene and dibenzothiophene by *Sphingomonas* sp LB126. *Res Microb* 154:199–206
- Vogt C, Losche A, Kleinstaub S, Muller S (2005) Population profiles of a stable, commensalistic bacterial culture grown with toluene under sulphate-reducing conditions. *Cytometry Part A* 66A:91–102
- Wick LY, de Munain AR, Springael D, Harms H (2002) Responses of *Mycobacterium* sp. LB501T to the low bioavailability of solid anthracene. *Appl Microb Biot* 58:378–385
- Wick LY, Mattle PA, Wattiau P, Harms H (2004) Electrokinetic transport of PAH-degrading bacteria in model aquifers and soil. *Environ Sci Technol* 38:4596–4602
- Wick LY, Shi L, Harms H (2007) Electro-bioremediation of hydrophobic organic soil-contaminants: a review of fundamental interactions. *Electrochim Acta* 52:3441–3448
- Wilson WW, Wade MM, Holman SC, Champlin FR (2001) Status of methods for assessing bacterial cell surface charge properties based on zeta potential measurements. *J Microbiol Methods* 43: 153–164
- Xu RL (1993) Methods to resolve mobility from electrophoretic laser-light scattering measurement. *Langmuir* 9:2955–2962